Journal of Hard Tissue Biology 31[2] (2022) 79-86

CODEN-JHTBFF, ISSN 1341-7649

Original

Evaluation of the Microstructural Characteristics of Bone Surrounding Anchor Screws Placed under a Horizontal Load by Exploring the Orientation of Biological Apatite Crystals and Collagen Fiber Anisotropy

Takaaki Matsumoto[1,2], Satoru Matsunaga[1,3], Masaaki Kasahara[4], Norio Kasahara[5], Takayoshi Nakano[6], Takuya Ishimoto[6] and Yasushi Nishii[2]

[1] *Oral Health Science Center, Tokyo Dental College, Tokyo, Japan*
[2] *Department of Orthodontics, Tokyo Dental College, Tokyo, Japan*
[3] *Department of Anatomy, Tokyo Dental College, Tokyo, Japan*
[4] *Department of Dental Materials Science, Tokyo Dental College, Tokyo, Japan*
[5] *Department of Histology and Developmental Biology, Tokyo Dental College, Tokyo, Japan*
[6] *Division of Materials & Manufacturing Science, Graduate School of Engineering, Osaka University, Osaka, Japan*
(Accepted for publication, February 16, 2022)

Abstract: The objective of this study was to carry out quantitative evaluations of the microstructural characteristics of bone surrounding anchor screws placed under a horizontal load and the microstructural characteristics of bone on the compressed and non-compressed sides of anchor screws by investigating the orientation of biological apatite (BAp) crystals and collagen fiber anisotropy. Anchor screws were implanted in the femurs of adult rats. They were divided into those placed under a horizontal load (horizontal loading group, $n = 4$), those not placed under a horizontal load (unloaded group, $n = 4$), and a sham group of rats that did not undergo femoral anchor screw implantation. In addition to histological observations, BAp crystal orientation and collagen fiber anisotropy were also analyzed. Osteocytes adjacent to anchor screws on the compressed side in the horizontal loading group were rounder in shape than those in normal femurs, the unloaded group, and on the non-compressed side in the horizontal loading group. Collagen fibers showed anisotropy on the non-compressed side in the horizontal loading group. BAp crystals also showed a uniaxial preferential orientation in the direction of traction on the compressed side in the horizontal loading group. These results demonstrated that the osteogenesis of bone around anchor screws placed under a sustained horizontal load gave this bone structural characteristics that differed in some respects from those of normal bone. They also showed that this bone acquired micro/nanostructural characteristics adapted to its new mechanical environment.

Key words: Anchor screw, Bone quality, Biological apatite crystal, Second harmonic generation images

Introduction

In recent years, orthodontic anchor screws have come into general use to provide stable anchorage in orthodontic treatment for dental or skeletal malocclusion[1-3]. In particular, they are now actively used for distal movement and intrusion of the molars, since adequate tooth movement is unlikely to be achieved by conventional orthodontic treatment[4,5]. According to Reynders *et al.*, however, the success rate of anchor screws during orthodontic treatment is 80%-90%, far lower than the reported success rate for dental implants of 96.7%-100%. Causes of anchor screw loss include poor oral hygiene, low bone density, insufficient cortical bone thickness, and the overload imposed on the anchor screw[6-9]. Numerous studies of dental implants have found that the load placed on the implant affects the outcome of implant treatment[10,11]. The absence of a periodontal ligament between dental implants and bone means that they lack a pressure-sensitive organ, and the tolerable vertical load is therefore known to be lower than that for natural teeth[12]. Dental implants have poor stability under horizontal load, and the superstructure must be adjusted to minimize as much as possible the load in this direction[13]. Anchor screws, however, provide the anchorage for tooth movement and are therefore placed under sustained horizontal load. It is thus important that anchor screws be retained in the jawbone and fulfill their role as anchors even under sustained horizontal load[14].

In the 1990s, when anchor screws first came into general use, studies by Melsen and Costa showed that, if anchor screws were placed under a horizontal load immediately after their insertion, the contact between bone and implant was uneven[15,16]. According to more recent orthodontic anchor screw guidelines, however, as long as the magnitude of the force is appropriate, it has no effect on the anchor screw loss rate in clinical use[17]. Despite these clinical data, there have been few detailed investigations of the condition of peri-implant bone and of bone quality factors in particular when a load has been applied immediately after insertion.

Although it is necessary to evaluate the relationship between the load condition of the anchor screw and the mechanical function of the bone, it is a very difficult task. Bone volume is generally used as a quan-

Correspondence to: Dr. Satoru Matsunaga, Department of Anatomy, Tokyo Dental College, 2-9-18, Kandamisaki-Cho, Chiyoda- Ku, Tokyo 101-0061, Japan; Tel: +81-3-6380-9592; Fax: +81-3-6380-9664; E-mail: matsuna@tdc.ac.jp

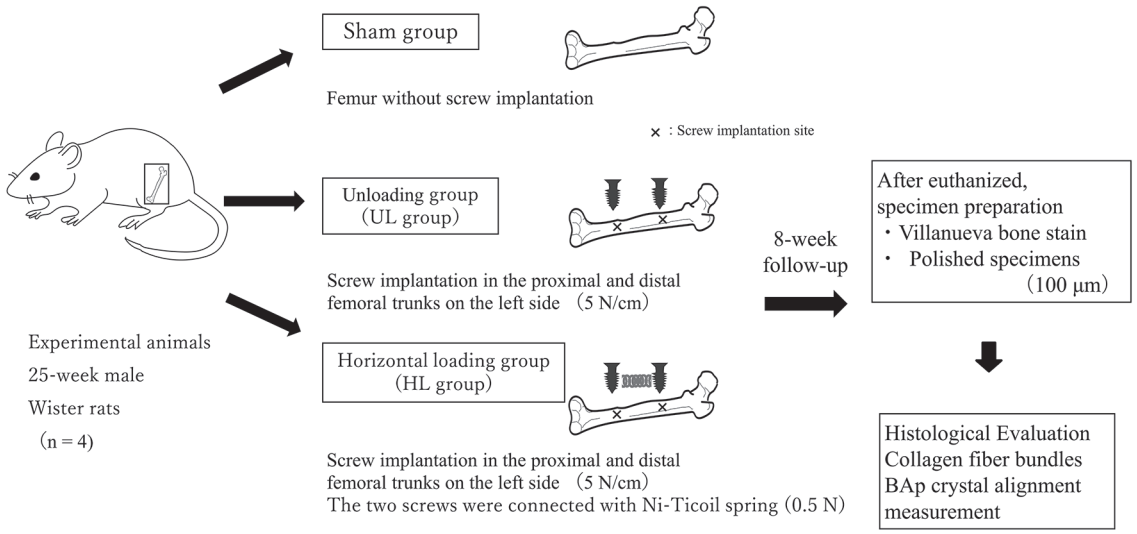

Figure 1. Experimental protocol. Anchor screws are implanted in the distal and proximal diaphyseal regions of the left femur. In the horizontal loading group (HL group, n = 4), these anchor screws are connected to each other with a coil spring to impose a lateral load. In the unloaded group (UL group, n = 4), nothing is connected to the anchor screws after implantation, leaving them free of lateral load. In the sham group (n = 4), sham surgery comprising a skin incision alone is performed on the femur, with no anchor screws implanted.

titative index of bone strength prior to dental implant treatment. Even with a large bone volume, however, implants are not necessarily successful[18]. Since the 2000 National Institutes of Health (NIH) Consensus Conference Statement, not only bone volume, but also bone quality factors have come to be regarded as playing an important biomechanical role in improving the success of dental implants[19]. Nakano *et al.* investigated the bone quality factors of biological apatite (BAp) crystal orientation and collagen fiber anisotropy, and they found that bone quality is strongly correlated with mechanical function[20]. On this basis, a detailed investigation of bone quality factors in the bone surrounding anchor screws and the identification of location-specific structural characteristics should enable the effect on bone mechanical function of the horizontal load applied to anchor screws to be predicted with high accuracy.

Therefore, the objective of this study was to carry out quantitative evaluations of the microstructural characteristics of bone surrounding anchor screws placed under a horizontal load and the microstructural characteristics of bone on the compressed and non-compressed sides of anchor screws by exploring the orientation of BAp crystals and collagen fiber anisotropy. The aim was to elucidate one aspect of the association between the mechanical environment and the microstructure of peri-implant bone.

Materials and Methods

Animal experiments were approved by the Tokyo Dental College Animal Experiment Committee (Ethics Application Number: 203110). Every possible effort was made to minimize animal suffering.

Experimental animals

Twelve adult, male, Wistar rats (age 25 weeks, mean weight 400 g) were used for this study. Anchor screws were implanted in the distal and proximal diaphyseal regions of the left femur. In the horizontal loading group (HL group, *n* = 4), these anchor screws were connected to each other with a coil spring to impose a lateral load (Fig. 1). In the unloaded group (UL group, *n* = 4), nothing was connected to the anchor screws after implantation, leaving them free of lateral load. In the sham group (*n* = 4), sham surgery comprising a skin incision alone was performed on the femur, with no anchor screws implanted.

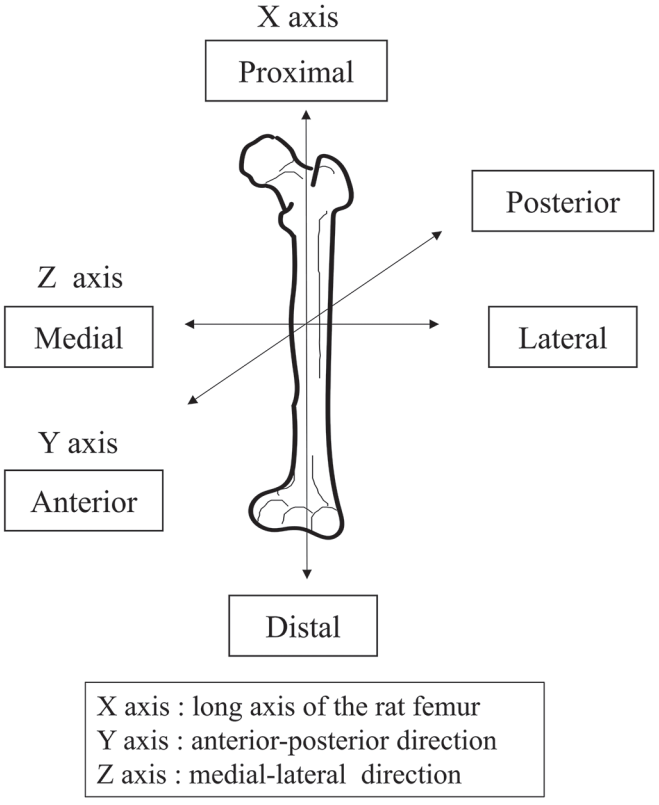

Figure 2. Axis definitions. The X axis is defined as the long axis of the femur, the Y axis as the anterior-posterior direction, and the Z axis as the medial-lateral direction.

The reference axes for the experimental specimens were defined as follows: X axis, long axis of the rat femur; Y axis, anterior-posterior direction; and Z axis, medial-lateral direction (Fig. 2).

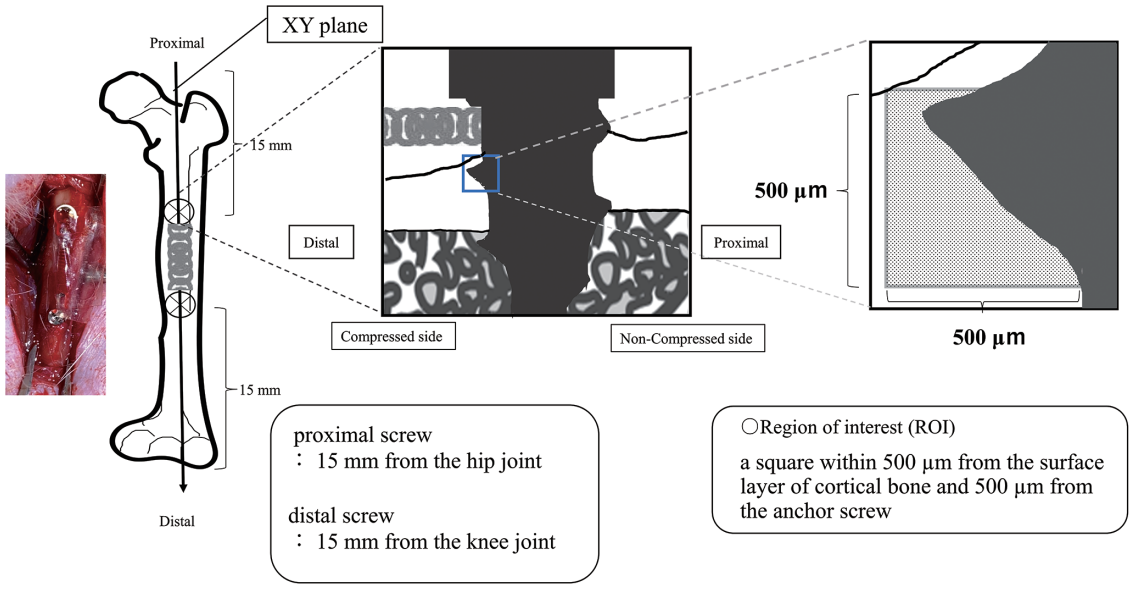

Figure 3. Region of interest (ROI) definition. The ROI is set at a depth of 500 µm from the surface layer of cortical bone, as a 500 µm × 500 µm square in the body of the anchor screw.

Surgical preparation

Anchor screw implantation was carried out under general anesthesia achieved by intraperitoneal administration of a mixture of three anesthetics (0.375 mg/kg medetomidine hydrochloride, Zenoaq, Fukushima, Japan; 2.0 mg/kg midazolam, Sandoz, Tokyo, Japan; and 2.5 mg/kg butorphanol tartrate, Meiji Seika Pharma, Tokyo, Japan). A skin incision measuring approximately 20 mm was made immediately above the left femur from the ventral side, and the muscle layers were divided to expose the bone. The periosteum was divided and detached, after which an orthodontic anchor screw (Le Forte system®, Jeil Medical Co, Seoul, Korea) was inserted above the periosteum in the direction of the Y axis at the anterior margin of the proximal metaphyseal region (15 mm from the hip joint) and the anterior margin of the distal metaphyseal region (15 mm from the knee joint) of the femur on each side, at a site with no muscle insertion in each case. The anchor screws used in this experiment were machined-surface, threaded, tapered screws of diameter 1.2 mm and length 3 mm, made of Ti-6Al-4V titanium alloy. A Ni-Ti coil spring (NT20-13U Dentos NT Coil Spring, Shofu, Kyoto, Japan) was attached to the anchor screws implanted in the left femur and adjusted to impose a sustained horizontal load of 0.5 N[21]. The muscle layers and skin were then sutured with 5-0 nylon thread to conclude the operation, and a medetomidine antagonist (0.75 mg/kg atipamezole hydrochloride, Zenoaq) was immediately administered intraperitoneally to maintain the rat's body temperature. After an 8-week healing period had elapsed following anchor screw implantation, the rats were euthanized, and both femurs were harvested.

Specimen preparation

Once all the femurs had been harvested, they were fixed by immersion in 10% buffered formalin at 4 °C for 2 days. Graded ethanol dehydration was performed, and prestaining was conducted with Villanueva Osteochrome Bone Stain (Funakoshi, Tokyo, Japan), after which the specimens were embedded in unsaturated polyester resin (Rigolac, Nisshin EM, Tokyo, Japan). They were then sliced with a rotating microtome (SP1600, Leica, Wetzlar, Germany) in the XY plane passing through the center of the two anchor screws. The slices were polished with waterproof abrasive paper (#400 to #800 to #1200) to produce 100-µm-thick polished specimens. These specimens were observed under a general-purpose optical microscope (Axiophot 2, Carl Zeiss, Oberkochen, Germany), the courses of blood vessels and osteoids were identified, and the morphology of the osteocytes around the anchor screws was analyzed with the packaged image-analysis software.

Measurement the morphology of osteocytes

Since osteocytes cannot be stained directly with Villanueva stain, the morphology of osteocytes was determined indirectly by examining the morphology of the bone cavities. The osteocytes were photographed at three different depths of focus in the region of interest (ROI), and the 20 osteocytes with the longest diameter were randomly measured. In addition, specimens with a long diameter of less than 6 µm were excluded. The ROI was set as a square within 500 µm from the surface layer of cortical bone and 500 µm from the anchor screw (Fig. 3). Osteocyte angles between the longest diameters of osteocytes and the long axes of peri-implant bone and normal bone were measured in the three groups. The longest and shortest diameters, with the latter defined as the diameter measured on a line passing through the center of the longest diameter and perpendicular to it, were measured at the location where the transverse diameter was greatest. Osteocyte angles were measured as the angle between the longest diameter of the osteocyte and the Y axis, with osteocytes with their longest diameter oriented parallel to the X axis defined as having an angle of 90°, those with their longest diameter oriented in the direction of the anchor screw head defined as having an angle of >90° with respect to the Y axis, and those with their longest diameter oriented in the direction of the anchor screw tip defined as having an angle of <90°.

Second harmonic generation imaging

Second harmonic generation (SHG) images were acquired using a multiphoton confocal microscopy system (LSM 880 Airy NLO; Carl Zeiss) with an excitation laser (Chameleon Vision II, wavelengths: 680-1,080 nm; repetition rate: 80 MHz; pulse width: 140 fs; Coherent Inc., Santa Clara, CA, USA) and an objective lens (Plan-Apochromat 10x/0.8

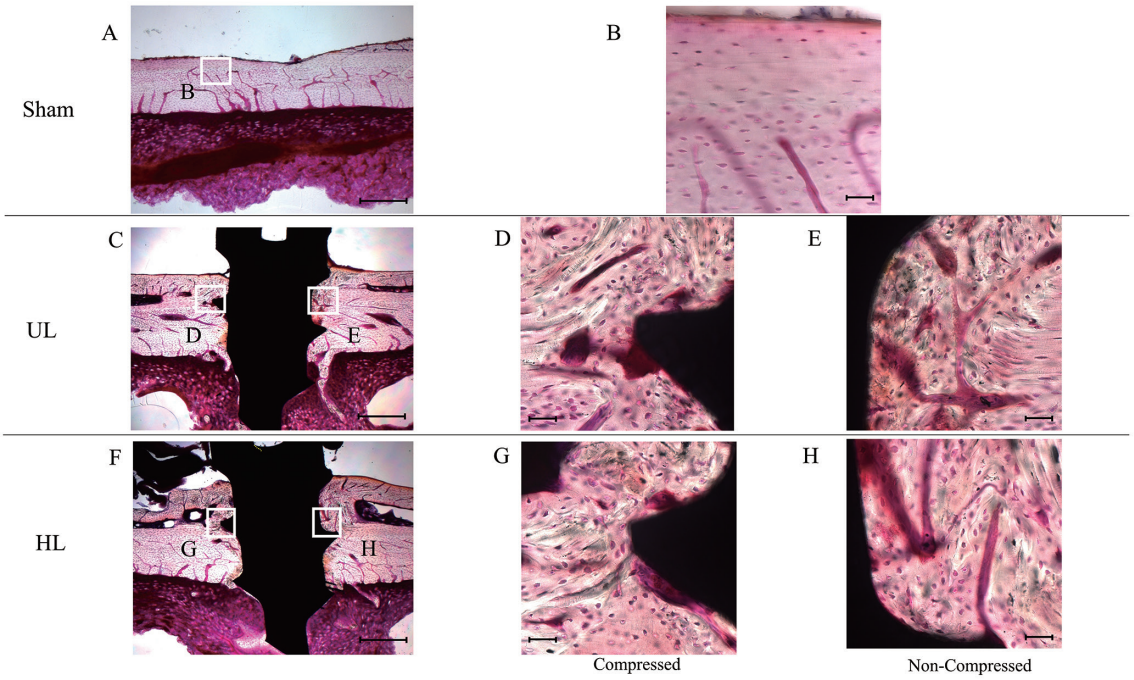

Figure 4. Villanueva-stained images. A. Sham group, low magnification. B. Sham group, high magnification. C. UL group, low magnification. D. UL group, mesial side of screw, high magnification. E. UL group, distal side of screw, high magnification. F. HL group, low magnification. G. HL group, compressed side, high magnification. H. HL group, non-compressed side, high magnification. In the UL and HL groups, the surface of the anchor screw is directly integrated with corticoid bone. (Fig. 4C, F). Numerous microvessels with irregular courses and irregularly arranged osteocytes are observed in the bone surrounding the anchor screws in the UL group and on both the compressed and non-compressed sides of the anchor screws in the HL group (Fig. 4D, E, G, H). Fig. 4A, C, F's scale bar: 500 μm. Fig. 4B, D, E, G, H's scale bar: 50 μm.

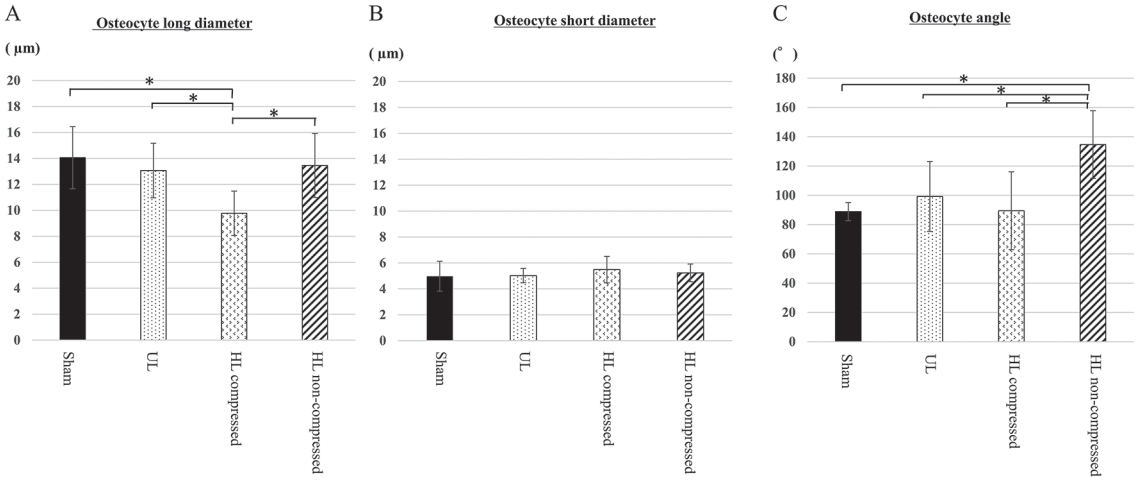

Figure 5. Osteocyte morphology and angle measurement. A. Osteocyte long diameter. B. Osteocyte short diameter. C. Osteocyte angle measurement. The long diameter of osteocytes is significantly shorter in the HL group than in the sham group, UL group, and HL non-compressed group. However, there is no significant difference in the short diameter; *p<0.05 compared to Sham.

M27; Carl Zeiss). The excitation wavelength for collagen fiber observation was 880 nm. Images were acquired using ZEN imaging software (Carl Zeiss). After image acquisition, the collagen fiber bundles in the ROI were traced using Imaris 8.4 software (Bitplane AG, Zurich, Switzerland), and their angles were measured.

BAp crystal alignment

BAp crystal alignment was analyzed by micro-region X-ray diffraction[21]. Measurements were made with a curved imaging-plate (IP) X-ray diffractometer (XRD: D/MAX PAPIDII-CMF, Rigaku Corporation, Tokyo, Japan) with two optical systems, a transmission optical system and a reflecting optical system. The measurements were compared with other ROIs and the same site, with Cu-Kα radiation used as the beam source in all cases. The tube voltage was 40 kV, and the tube current was 30 mA. The irradiation field was determined using the optical microscope fitted to the XRD (0.6–4.8× magnification), and the incident beam was a circular microbeam of diameter 100 μm. The transmission optical system was used for measurements in the X- and Y-axis direc-

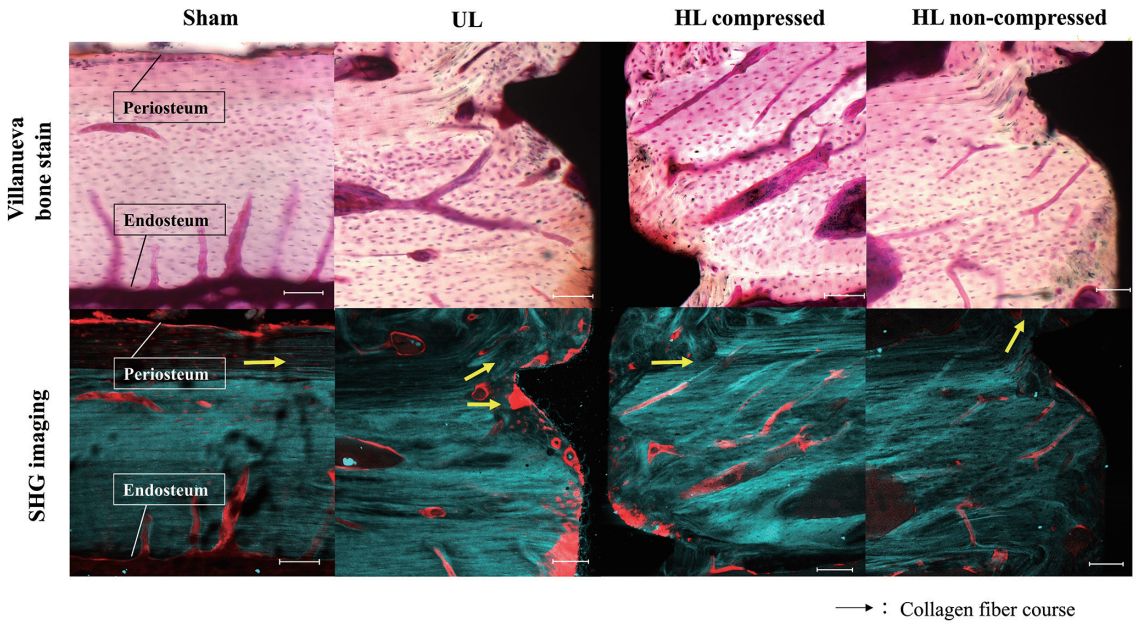

Figure 6. SHG images from around the screws in each group. The top row shows Villanueva staining, and the bottom row SHG imaging. On the non-compressed side in the HL group, there are large numbers of collagen fiber bundles around the anchor screw that run in the direction in which the anchor screw has been inserted (Y axis direction). Scale bar: 100 μm.

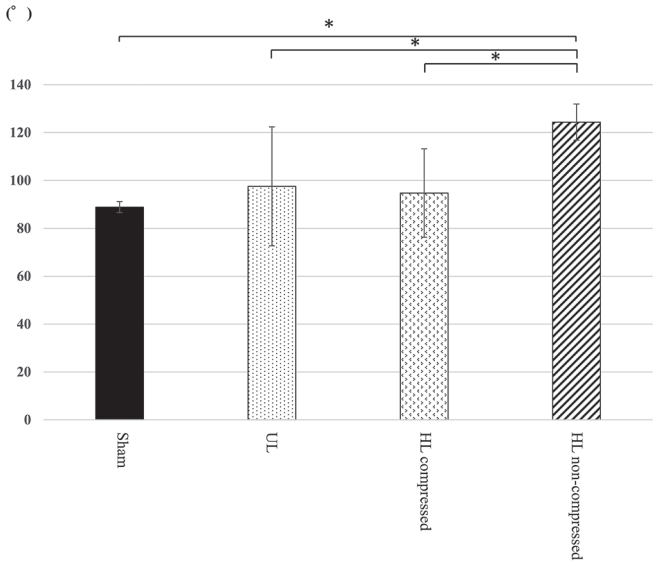

Figure 7. Angle measurements of collagen fibers in the superficial layer of peri-implant cortical bone. The angle is significantly larger on the uncompressed side; *p<0.05 compared to Sham.

tions, and the reflecting optical system was used for measurements in the Z-axis direction. Using 2D Data Processing software (Rigaku), the X-ray intensity ratios of the two diffraction peaks in the (002) and (310) planes were calculated from the diffraction X-ray beam detected using the curved IP. The X-ray diffraction intensity ratio for hydroxyapatite (HAp) powder measured using the transmission optical system was 3.01, and that using the reflecting optical system was 1.2.

Statistical analysis

Statistical analysis was conducted using Tukey's test to compare the mean values in the different groups, with $p < 0.05$ regarded as significant.

Results

Histological observation of peri-implant bone

Fig. 4 shows the results of the histological evaluations of the polished specimens (Villanueva Osteochrome Bone Stain) of peri-implant bone from the Sham, UL, and HL groups. In the UL and HL groups, the surface of the anchor screw was directly integrated with corticoid bone, with good osseointegration observed even under the horizontal load condition (Fig. 4C, F). However, numerous microvessels with irregular courses and irregularly arranged osteocytes were observed in the bone surrounding the anchor screws in the UL group and on both the compressed and non-compressed sides of the anchor screws in the HL group (Fig. 4D, E, G, H). An equivalent level of calcification to that seen in the cortical bone of the femoral shaft was observed in both groups.

Morphology of osteocytes

Fig. 5 shows the longest/shortest diameters of osteocytes and their angle measurements. In the normal rat femoral shaft, osteocytes were elliptical in shape, with a long:short diameter ratio of approximately 3:1, and the long diameters were oriented in almost exactly the same direction as X axis on the XY plane (Fig. 5). In the peri-implant bone, however, although there was no significant difference in osteocyte short diameter between any of the groups, the long diameter was significantly shorter on the compressed side in the HL group than in the other groups. The osteocyte angle was significantly higher on the non-compressed side in the HL than in the other groups.

Anisotropy of collagen fiber orientation

Fig. 6 shows the courses of collagen fibers in peri-implant bone as shown by Villanueva staining and SHG imaging at the same site. Laminar structures of collagen fiber bundles running parallel to the periosteum and endosteum were evident in the peri-implant bone in all groups. This was the same orientation as that of the long axis of the femurs with

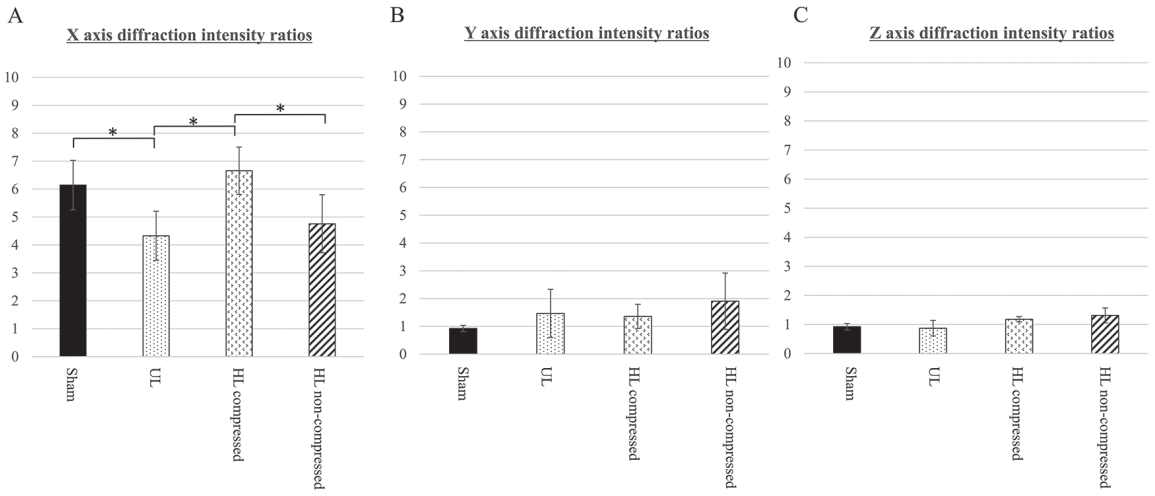

Figure 8. Diffraction intensity ratios in each axis. A. X axis diffraction intensity ratios. B. Y axis diffraction intensity ratios. C. Z axis diffraction intensity ratios. The diffraction intensity ratio in the X axis direction is significantly higher on the compressed side in the HL group than on the non-compressed side in the HL group or in the Sham and UL groups; *p<0.05 compared to Sham.

no anchor screw inserted. At the anchor screw-bone interface, however, their courses were disrupted in a few places. On the non-compressed side in the HL group, there were large numbers of collagen fiber bundles around the anchor screw that ran in the direction in which the anchor screw had been inserted (Y axis direction). Fig. 7 shows the results of the statistical analysis of the angle between collagen fibers and the Y axis in peri-implant bone. The angle of orientation of collagen fiber bundles in the ROI was significantly larger on the non-compressed side in the HL group than in any of the other groups.

BAp crystal alignment

Fig. 8 shows the X-ray diffraction intensity ratios in the areas of peri-implant bone where measurements were made in the (002) and (310) planes. In all groups, a uniaxial preferential orientation in the X axis direction was observed (Fig. 8A). The diffraction intensity ratio was also significantly higher on the compressed side in the HL group than on the non-compressed side in the HL group or in the Sham and UL groups. In the Y-axis and Z-axis directions, however, BAp crystals did not show a preferential orientation in any of the groups (Fig. 8B, C).

Discussion

The present histological observations showed a distinctive feature of the orientation of blood vessels in peri-implant bone. Intraosseous vessels around anchor screws are generated with irregular orientations, a major difference from the laminar bone structure of normal rat femurs in which the vessels extend from the endosteum toward the periosteum. This suggests that anchor screw implantation causes angiogenesis to vary from that seen in the normal femur. The fact that there was a similar tendency in the courses of the blood vessels between the HL and UL groups suggests that a horizontal load has little effect on angiogenesis. The results of the histological observations in this study did not show any signs of diminished anchor screw stability, such as gaps between the anchor screws and the surrounding bone or bone resorption around the anchor screws, in either the UL group or the HL group that underwent anchor screw implantation.

The osteocytes around the anchor screws in the Sham group and UL group and on the non-compressed side in the HL group were all long, thin ellipses, similar to the osteocytes in normal femoral bone. On the compressed side in the HL group, however, the long diameter of the osteocytes was significantly shorter, and the ellipses were rounder in shape. The angle between the long diameter of the osteocytes and Y axis was close to 90° in the Sham group and UL groups, and on the compressed side in the HL group, but on the non-compressed side in the HL group, it was significantly larger, at 130°. Robling *et al.* carried out *in vitro* experiments on morphological changes in osteocytes, and they found that both their morphology and stiff cytoskeleton changed as a result of the mechanical environment[22]. The present results were similar, confirming that the horizontal load imposed on anchor screws generates compressive stress that also affects osteocyte morphology under *in vivo* conditions.

With respect to the orientation of collagen fiber bundles in peri-implant bone, the results of SHG imaging confirmed that almost all collagen fiber bundles ran parallel to the long axis of the femur in the Sham group and UL groups and on the compressed side of the HL group. The collagen fiber bundles in normal rat femoral bone run in the direction of the long axis of the femur. This demonstrated that, when bone is regenerated during the healing process after screw implantation, the collagen fiber bundles are repaired with the same orientation as in normal femoral cortical bone. On the non-compressed side in the HL group, however, numerous collagen fiber bundles were observed to run either perpendicular to the orientation of normal collagen fiber bundles or at a more obtuse angle to them. Collagen fiber bundle orientation is a factor that resists the tensile stress on the bone, and severe tensile stress may have been generated on the non-compressed side in the HL group[20]. In addition, these results resemble those for the arrangement of osteocytes on the non-compressed side in the HL group. The femur of the rat is made up of lamellar bone, and the collagen fibers run parallel to the lamellar bone. Since the direction of the long axis of bone cells is arranged parallel to the lamellar bone, it is considered that the arrangement of bone cells and the running of the collagen fiber bundles were similar.

BAp crystal alignment exhibited a uniaxial preferential orientation in the direction of the long axis of the femur (the X axis direction) in all groups. This suggested that anchor screw implantation did not generate sufficient stress in the bone to change the principal stress direction. However, a comparison of the diffraction intensity ratio in the X axis direction found that it was significantly higher on the compressed side in

the HL group than in either the control and UL groups or on the non-compressed side in the HL group. We conjectured that, because the horizontal load was constantly imposed in the X axis direction, the bone compressed by the anchor screws resisted the compressive load, giving it a more pronounced preferential orientation than normal. There was no significant difference in preferential orientation between the Sham group and UL groups or the non-compressed side in the HL group. This demonstrated that the compressed side of the peri-implant bone, which lacks an intervening periodontal membrane, is under a particularly high compressive load. This suggests that, the greater the horizontal load, the greater the compressive stress imposed on the compressed side of the peri-implant bone, and this may contribute to anchor screw loss.

In the experimental model used in the present study, the horizontal load was imposed immediately after anchor screw implantation to avoid subjecting the rats to multiple invasive surgeries. Manni *et al.* conducted a clinical study of the immediate loading of anchor screws, and they reported that, as long as osseointegration of the peri-implant bone was achieved, the anchor screw provided stable anchorage without falling out, even if a horizontal load were imposed immediately after insertion without an intervening healing period[23]. However, that study neither indicated a specific success rate nor described the effect on peri-implant bone. Luzi *et al.* conducted animal experiments on the immediate loading of anchor screws, and they found that, although the volume of peri-implant bone was slightly greater when a horizontal load was not applied during the healing period, there were no significant differences in the mineralizing surface, bone-to-implant contact rate, or erosion surface, and there was no effect on anchor screw stability[24]. In the present study, it was also found that the immediate imposition of a horizontal load had no effect on anchor screw stability, with no loosening or loss observed. This suggests that immediate loading does not adversely affect the stability of anchor screws.

Because this was a study of the bone reaction to horizontal load, the magnitude of this load was set so as not to result in anchor screw loss. At this level of load, however, it was not possible to investigate the bone reaction when an excessively large horizontal load is applied to an anchor screw, causing it to fall out. Although the peri-implant bone did show a bone reaction in response to the mechanical environment created by a horizontal load of the magnitude applied in this study, it was not possible to investigate changes in this bone reaction in response to changes in the magnitude of horizontal load. In terms of timing, too, using the present experimental model, it was only possible to investigate the effect of loading immediately after implantation. Therefore, early loading and late loading could not be compared. Further experiments with loads of different magnitudes applied at different times are required to investigate subsequent changes in peri-implant bone.

The results of the present study demonstrated that, although the osteogenesis that occurred in bone surrounding anchor screws subjected to a sustained horizontal load gave this bone structural characteristics that differed in some respects from those of normal bone; it acquired micro/nanostructural characteristics that were adapted to its new mechanical environment. This suggests that, although horizontal load is considered to be a high-risk factor for dental implants, peri-implant bone is capable of adapting, and bone in sufficiently good condition to provide absolute anchorage can be obtained.

Acknowledgments

This study was supported by a research grant from the Japan Society for the Promotion of Science (contract grant number: 18K09643,17K11808) and was partly supported by a grant from the Multidisciplinary Research Center for Jaw Disease (MRCJD): Achieving Longevity and Sustainability by Comprehensive Reconstruction of Oral and Maxillofacial Functions.

Conflict of Interest

The authors have no conflict of interest to report.

References

1. Liu Y, Yang Z, Zhou J, Xiong P, Wang Q, Yang Y, Hu Y and Hu J. Comparison of anchorage efficiency of orthodontic mini-implant and conventional anchorage reinforcement in patients requiring maximum orthodontic anchorage: A systematic review and meta-analysis. J Evid Based Dent Pract 20: 101401, 2020
2. Papadopoulos MA, Papageoorgiou SN and Zogakis IP. Clinical effectiveness of orthodontic mini-screw implants: a meta-analysis. J Dent Res 90: 969-976, 2011
3. Kuroda S, Yamada K, Deguchi T, Kyung HM and Takano-Yamamoto T. Class II malocclusion treated with mini-screw anchorage: Comparison with traditional orthodontic mechanics outcomes. Am J Orthod Dentofacial Orthop 135: 302-309, 2009
4. Mohamed RN, Basha S and Al-Thomali Y. Maxillary molar distalization with mini-screw-supported appliances in Class II malocclusion: A systematic review. Angle Orthod 88: 494-502, 2018
5. Kim DH and Sung SJ. Nonsurgical correction of a Class III skeletal anterior open-bite malocclusion using multiple micro-screw implants and digital profile prediction. Am J Orthod Dentofacial Orthop 154: 283-293, 2018
6. Reynders R, Ronchi L and Bipat S. Mini-implants in orthodontics: A systematic review of the literature. Am J Orthod Dentofacial Orthop 135: 564. E1-19, 2009
7. Nkenke E and Fenner M. Indications for immediate loading of implants and implant success. Clin Oral Implants Res 17: 19-34, 2006
8. Alharbi F, Almuzian M and Bearn D. Miniscrews failure rate in orthodontics: Systematic review and meta-analysis. Eur J Orthod 40: 519-530, 2018
9. Ramírez-Ossa DM, Escobar-Correa A, Ramírez-Bustamante MA and Agudelo-Suárez AA. An umbrella review of the effectiveness of temporary anchorage devices and the factors that contribute to their success or failure. J Evid Based Dent Pract 20: 101402, 2020
10. Heiderich CMC, Tedesco TK, Netto SS, de Sousa RC, Allegrini Júnior S, Mendes FM and Gimenezac T. Methodological quality and risk of bias of systematic reviews about loading time of multiple dental implants in totally or partially edentulous patients: An umbrella systematic review. Jpn Dent Sci Rev 56: 135-146, 2020
11. Chen J, Cai M, Yang J, Aldhohrah T and Wang Y. Immediate versus early or conventional loading dental implants with fixed prostheses: A systematic review and meta-analysis of randomized controlled clinical trials. J Prosthet Dent 122: 516-536, 2019
12. Demenko V, Linetskiy I, Nesvit K and Shevchenko A. Ultimate masticatory force as a criterion in implant selection. J Dent Res 90: 1211-1215, 2011
13. Meijer HJA, Boven C, Delli K and Raghoebar GM. Is there an effect of crown-to-implant ratio on implant treatment outcomes? A systematic review. Clin Oral Implants Res 29: 243-252, 2018
14. Migliorati M, Drago S, Gallo F, Amorfini L and Dalessandri D. Immediate versus delayed loading: comparison of primary stability loss after miniscrew placement in orthodontic patients—a singlecentre blinded randomized clinical trial. Eur J Orthod 38: 652-659, 2016

15. Costa A, Raffaini M and Melsen B. Miniscrews as orthodontic anchorage: a preliminary report. AOOS 13: 201-209, 1998
16. Melsen B and Costa A. Immediate loading of implants used for orthodontic anchorage. Clin Orthod Res 3: 23-28,2000
17. Chopra SS and Chakranarayan SLCA. Clinical evaluation of immediate loading of titanium orthodontic implants. Med J Armed Forces India 71: 165-170, 2015
18. Marshall D, Johnell O and Wedel H. Meta-analysis of how well measures of bone mineral density predict occurrence of osteoporotic fractures. BMJ 312: 1254-1259, 1996
19. NIH Consensus Development Panel on Osteoporosis Prevention, Diagnosis, and Therapy, Osteoporosis prevention, diagnosis, and therapy. JAMA 285: 785-795, 2001
20. Nakano T, Kaibara K, Tabata Y, Nagata N, Enomoto S, Marukawa E and Umakoshi Y. Unique alignment and texture of biological apatite crystallites in typical calcified tissues analyzed by microbeam X-ray diffractometer system. Bone 31: 479-487, 2002
21. Motoyoshi M, Inaba M, Ono A, Ueno S and Shimizu N. The effect of cortical bone thickness on the stability of orthodontic mini-implants and on the stress distribution in surrounding bone. Int J Oral Maxillofac Surg 38: 13-18, 2009
22. Robling AG and Bonewald LF. The osteocyte: New insights. Annu Rev Physiol 82: 485-506, 2020
23. Manni A, Cozzani M, Tamborrino F and De Rinaldis S. Factors influencing the stability of miniscrews. A retrospective study on 300 miniscrews. Eur J Orthod 33: 388-395, 2011
24. Luzi C, Verna C and Melsen B. Immediate loading of orthodontic mini-implants: A histomorphometric evaluation of tissue reaction. Eur J Orthod 31: 21-29, 2009